

Compromised Cytoarchitecture and Polarized Trafficking in Autosomal Dominant Polycystic Kidney Disease Cells

Audra J. Charron,* Sakie Nakamura,† Robert Bacallao,§ and Angela Wandinger-Ness||

*Integrated Graduate Program in the Life Sciences, †Department of Medicine, Northwestern University Medical School, Chicago, Illinois 60611; §Department of Medicine, Indiana University Medical Center, Indianapolis, Indiana 46202; and

||Department of Pathology, University of New Mexico Health Sciences Center, Albuquerque, New Mexico 87131

Abstract. Cystogenesis associated with autosomal dominant polycystic kidney disease (ADPKD) is characterized by perturbations in the polarized phenotype and function of cyst-lining epithelial cells. The polycystins, the protein products of the genes mutated in the majority of ADPKD cases, have been described recently, but the pathological mechanism by which causal mutations result in the mislocalization of cell membrane proteins has remained unclear. This report documents the dissociation from the ADPKD cell basolateral membrane of three molecules essential for spatial organization and exocytosis. The adherens junction protein E-cadherin, the subcellular disposition of which governs intercellular and intracellular architecture, was discovered sequestered in an internal ADPKD cell compartment. At the same time, sec6 and sec8, components of a complex critical for basolateral cargo deliv-

ery normally arrayed at the apico-lateral apex, were depleted from the ADPKD cell plasma membrane. An analysis of membrane transport revealed that basolateral trafficking of proteins and lipids was impaired as a result of delayed cargo exit from the ADPKD cell Golgi apparatus. Apical transport proceeded normally. Taken together with recent documentation of an association between polycystin-1 and E-cadherin (Huan and van Adelsberg, 1999), the data suggest that causal mutations disrupt E-cadherin-dependent cytoarchitecture, adversely affecting protein assemblies crucial for basolateral trafficking.

Key words: basolateral • adherens junction • epithelia • autosomal dominant polycystic kidney disease (ADPKD) • polycystin

Introduction

The efficacy with which epithelial cells absorb, filter, and secrete metabolites is predicated upon a polarized cell architecture and vectorial molecular trafficking (Yeaman et al., 1999). Autosomal dominant polycystic kidney disease (ADPKD)¹ is a common inherited disease characterized by numerous morphological and functional alterations, many of which may be explained by deficits in the

cyst epithelial cell differentiation program. The aberrant expression of select basolateral proteins on the apical ADPKD cell surface (Wilson, 1997) is associated with the progressive accumulation and enlargement of fluid-filled cysts, which ultimately abrogates renal function (Carone et al., 1994). Although it has long been supposed that modulations in cytoarchitecture and the fidelity of molecular targeting are central to ADPKD pathology (for review see Wilson, 1997), a mechanistic link between the occurrence of causal mutations and dysmorphogenesis has yet to be discovered.

Recent progress concerning the genes responsible for ADPKD has been instrumental in identifying the molecular genetic basis of this disorder. Genetic lesions associated with >85% of ADPKD cases have been mapped to the polycystic kidney disease (PKD) 1 gene (Reeders et al., 1985), whereas the remaining cases are due to mutations in PKD2 (Mochizuki et al., 1996), and in rare instances a third undescribed locus (Daoust et al., 1995). The PKD1 and PKD2 genes encode polycystin-1 and polycystin-2, re-

This study is the result of collaborative efforts between two laboratories. R. Bacallao and A. Wandinger-Ness contributed equally to the supervision of the experiments herein.

Address correspondence to Angela Wandinger-Ness, 2325 Camino de Salud CRF 225, Department of Pathology, University of New Mexico Health Sciences Center, Albuquerque, NM 87131-5301. Tel.: (505) 272-1459. Fax: (505) 272-4193. E-mail: wness@unm.edu

¹Abbreviations used in this paper: ADPKD, autosomal dominant polycystic kidney disease; AEBSEF, 4-(2-aminoethyl) benzenesulfonyl fluoride; HCl; HA, hemagglutinin; HMEM, HEPES-buffered MEM; LDL-R, low density lipoprotein receptor; pAb, polyclonal antibody; PKD, polycystic kidney disease; SNARE, soluble N-ethylmaleimide-sensitive attachment protein receptor; TX, Triton X.

spectively (Hughes et al., 1995; International Polycystic Kidney Disease Consortium, 1995; Mochizuki et al., 1996). The clinically salient onset of ADPKD during mid-life is attributable to the acquisition of a second (somatic) mutation at the PKD1 or PKD2 loci (Qian et al., 1996; Koptides et al., 1999), which serves as the primary pathogenic stimulus that precipitates deterioration of previously normal epithelial tissue. Singular homozygous mutant cells are thought to undergo partial dedifferentiation and proliferation, leading to repopulation of the tubule wall and development of a clonal cyst (Carone et al., 1994; Qian et al., 1996).

Analyses describing protein topology and intermolecular interactions have yielded important information regarding the localization and potential roles of the polycystins. Polycystin-1 is a 480,000-mol wt putative transmembrane protein (Hughes et al., 1995; International Polycystic Kidney Disease Consortium, 1995) localized solely along lateral contacting membranes of cultured cells (Ibraghimov-Beskrovnya et al., 1997). A predicted 2,500-amino acid extracellular domain is comprised of diverse motifs with putative functions in cell-cell and cell-extracellular matrix interactions (Hughes et al., 1995; International Polycystic Kidney Disease Consortium, 1995; Moy et al., 1996), suggesting that polycystin-1 plays a role in adhesion (Hughes et al., 1995). Polycystin-2 is an integral membrane protein consisting of domains with significant homology to polycystin-1 as well as to a family of voltage-gated ion channels (Mochizuki et al., 1996). Polycystin-1 and polycystin-2 interact physically via their COOH termini (Qian et al., 1997; Tsiokas et al., 1997), offering an explanation for the observation that mutations in either gene results in an identical phenotype (Tsiokas et al., 1997). Despite this progress, uncertainties regarding the molecular mechanism whereby alterations in the polycystins influence the phenotype of ADPKD cells have persisted. An exciting insight was provided by the recent description of intermolecular interactions between endogenous cellular polycystin-1 and E-cadherin, the integral membrane component of epithelial adherens junctions (Huan and van Adelsberg, 1999).

E-cadherin is critical for the institution and perpetuation of epithelial cell polarity on account of its well-established role in the stabilization and elaboration of cytoskeletal-junctional complexes, and its more recently defined function in basolateral targeting patch recruitment (Yeaman et al., 1999). Initial E-cadherin-mediated epithelial cell adhesion is instrumental in reorganizing the cytoskeleton and exocytic transport machinery, and in establishing an apico-basolateral pole. The formation of tight junctions and the polarized delivery of vesicles and their cargo to newly defined apical and basolateral surfaces result in the genesis of two biochemically unique membrane domains. Because distinct vesicles carrying segregated apical and basolateral cargo are generated in fibroblasts as well as epithelial cells (Yoshimori et al., 1996), minimal maturation of the Golgi apparatus may be required during epithelial differentiation, and the differentiating cell is likely competent to engage in vectorial trafficking as soon as vesicle targeting sites at the plasma membrane are delineated. Specification of these targeting sites occurs in response to E-cadherin-mediated adhesion. As intercellular E-cad-

herin interactions stabilize cytoskeletally tethered membrane proteins, a subset of cytosolic proteins are recruited to the contacting membranes. The sec proteins comprising the multimeric exocyst (TerBush et al., 1996) are among those cytosolic proteins recruited to the basolateral membrane in response to E-cadherin ligation (Grindstaff et al., 1998). These proteins demarcate a basolateral targeting patch that cooperates with the soluble *N*-ethylmaleimide-sensitive attachment protein receptor (SNARE) family of vesicular and target membrane receptors to ensure the proficiency of basolateral trafficking (Grindstaff et al., 1998). The maintenance of this highly defined cellular organization is crucial in the continued performance of epithelial tissues.

Because E-cadherin is critical for epithelial cell organization, it is interesting to consider the possibility that mutations in PKD1 or PKD2 disrupt normal E-cadherin-polycystin assemblies, and consequently impact ADPKD cell morphology and performance. Therefore, an assessment of ADPKD cell architecture and molecular trafficking was undertaken in order to identify specific derangements that lead to the compromised phenotypic state typical of these cells.

Materials and Methods

Chemical Reagents and Antibodies

Super Signal chemiluminescent substrate was supplied by Pierce. 4-(2-aminoethyl) benzenesulfonyl fluoride, HCl (AEBSF) and Mowiol 4-88 were obtained from Calbiochem. Unless otherwise stated, all other chemical reagents were obtained from Sigma Chemical Co. Mouse mAbs against E-cadherin and rSec8 were purchased from Transduction Laboratories. A rabbit polyclonal antibody (pAb) against the COOH terminus of PR8 hemagglutinin (HA) has been described previously (Wandinger-Ness et al., 1990). A mouse mAb against sec6 was purchased from Stressgen Biotechnologies Corp. A rabbit pAb against occludin was supplied by Zymed Immunochemicals. Mouse mAbs against human low-density lipoprotein receptor (LDL-R) (Van Driel et al., 1989) and p75^{NTR} (US Patents 4,786,593 and 4,855,241) were amplified as ascites (Harlow and Lane, 1988) using CRL-1898 and HB-8737 hybridoma cells (American Type Culture Collection), respectively. Fluorophore-conjugated secondary antibodies were purchased from Vector Laboratories, a rabbit pAb directed against mouse IgG used as a linker antibody was obtained from Jackson ImmunoResearch, and HRP-conjugated antibodies were bought from Amersham Pharmacia Biotech.

Cell Culture

Normal kidneys were obtained from previously healthy individuals whose acute injuries precluded organ transplantation. ADPKD kidneys were obtained after their surgical removal in preparation for transplant when patients were diagnosed with end-stage renal failure as a result of advanced ADPKD. Individual proximal tubule-derived cysts from ADPKD kidneys or proximal tubules from normal kidneys were isolated and dissected. The epithelial layer was separated from the underlying connective tissue layer and the epithelial cells isolated as described (Carone et al., 1989). Cultures were maintained in a humidified atmosphere of 5% CO₂ at 37°C. Cells for experiments were plated at a density of 300,000 cells per 24 mm² cell culture filter insert (0.4- μ m pore size) (Falcon; Becton Dickinson). Falcon tissue culture inserts were chosen based on the physical integrity of the inserts, vigorous cell growth, and morphological similarity between the two cell types. Cells were fed every other day with fresh medium until they were used for experiments on the fifth day after plating. After 5 d in culture, the integrity of all cell monolayers was assayed by light microscopy and the transepithelial resistance of select filters was measured. Once confluence was reached at culture day 3, the cells maintained a transepithelial resistance of \sim 250 ohms/cm², measured using a chopstick ohmmeter (World Precision Instruments). When used for im-

munofluorescence experiments, cells were also costained for the tight junction marker occludin to visually demonstrate cell confluence. Every experiment described in this study was performed in triplicate, using primary cells derived from normal or polycystic kidneys, in each case from three unrelated patients. The same patient samples (expanded no further than passage 4) were used throughout the study to minimize any effects of phenotypic variation.

Fluorescent Lipid Transport Assay

250 nmol C₆-NBD-ceramide (Molecular Probes) in chloroform and methanol was dried to a powder under dry nitrogen and prepared as a BSA complex as described (Pagano, 1989). The methods used to label live cells with C₆-NBD-ceramide and monitor lipid transport were based on published procedures (Lipsky and Pagano, 1985; van Meer et al., 1987). Immediately before the experiment, an aliquot of prepared C₆-NBD-ceramide was thawed and diluted 1:3 in phenol red-free Hepes-buffered MEM (HMEM) containing 0.35 g/liter NaHCO₃ and 60 mg/liter KH₂PO₄ (HMEM_{bath}). Filter-grown cells were rinsed twice with PBS⁺ and 300 μl of the diluted fluorescent lipid was applied to the apical surface, whereas 2 ml of HMEM_{bath} equilibrated to 20°C was applied to the basolateral surface. Cells were incubated in a 20°C darkened water bath for 90 min to allow lipid accumulation in the Golgi apparatus. The cells were then rinsed twice in ice-cold PBS⁺ and cell surface lipids were removed by two incubations for 15 min each in a 10°C water bath with HMEM_{bath} containing 5 mg/ml delipidated BSA. Cell surface transport of Golgi-accumulated lipids was initiated by adding prewarmed (37°C) phenol red-free HMEM containing 3.7 g/l NaHCO₃ and 60 mg/l KH₂PO₄ (1 ml apical, 2 ml basolateral). Subsequently, cells were incubated from 0–90 min at 37°C in a humidified 5% CO₂ incubator. At the appropriate time, filter inserts were excised from the plastic holder with a scalpel. The filter was mounted cell side up on an ice-cold microscope slide with PBS⁺ and a coverslip, and confocal images were collected immediately.

Immunofluorescence Microscopy

Filter inserts were rinsed in PBS, then fixed for 20 min at room temperature with 3% (wt/vol) paraformaldehyde, 0.1% (vol/vol) Triton X (TX)-100 (Fluka) prepared in PBS containing 1 mM CaCl₂ and 1 mM MgCl₂ (PBS⁺). Reactive aldehyde sites were quenched by incubation in 50 mM NH₄Cl prepared in PBS⁺ for 20 min at room temperature. Nonspecific binding sites were blocked by incubation in PBS containing 0.2% (vol/vol) fish skin gelatin (Sigma Chemical Co.) for 30 min at room temperature. Insert supports were excised and cut into conveniently sized pieces. These pieces were incubated in primary antibody diluted in PBS containing 0.2% (vol/vol) fish skin gelatin for 1 h at 37°C in a humidified chamber. Samples were rinsed with three changes of PBS and incubated with the appropriate fluorophore-conjugated secondary antibody for 30 min at 37°C. Insert sections were washed twice for 15 min each with PBS and mounted between nail polish support posts in Mowiol 4-88. Cells were either viewed on a Zeiss Universal epifluorescence microscope or imaged using a Zeiss LSM 510 inverted laser scanning microscope equipped with He-Ne and Kr-Ar lasers. For the sec6/8 localization, several 0.4-μm-thick images taken from the cell apex to the basal substrate were assembled as an extended-focus image. For the localization of E-cadherin, epifluorescence profiles as well as images from one basolateral focal plane are shown. Cells examined during the fluorescent lipid transport assay were imaged at a single focal plane along the basolateral cell surface.

Electron Microscopy

Cells grown on filters were washed in PBS and then fixed in 2.5% (wt/vol) glutaraldehyde in 0.1 M sodium cacodylate buffer, pH 7.4, for 1 h. After three rinses in 0.1 M sodium cacodylate buffer, the cells were postfixed in 1% (wt/vol) aqueous OsO₄ for 1 h at room temperature. The cells were rinsed in distilled water and stained with 1% (wt/vol) aqueous uranyl acetate in the dark for 1.5 h. The cells were dehydrated in a graded ethanol series, infiltrated, and embedded in Spurr's resin. Ultrathin sections were cut to 80 nm on a MT 6000-XL ultramicrotome (Ventana RMC), collected on 300 mesh nickel grids, stained with 2% (wt/vol) aqueous uranyl acetate for 4 min followed by 0.4% (wt/vol) lead citrate for 4 min. The sections were viewed on a Philips CM 120 electron microscope.

Influenza Infection

Wild-type influenza (A/PR/8/34) virus stocks were grown in embryonated chicken eggs as described (Kuchler, 1977). Filter-grown cells were rinsed

with PBS and infected with influenza virus at 10 pfu/cell for 1 h at 37°C. The virus was diluted in DME with 0.2% BSA (DME/BSA) and 300 μl was added to the apical surface, whereas 3 ml of the same medium without virus was added basolaterally. After the 1-h virus adsorption phase, cells were washed and incubated for 4 h at 37°C in DME/BSA before either metabolic labeling or steady-state biotinylation assays.

Recombinant Adenovirus Infection

Recombinant adenoviruses encoding either LDL-R or p75^{NTR} were kindly provided by Drs. Joachim Herz (University of Texas Southwestern Medical Center, Dallas, TX) (Herz and Gerard, 1993) and Moses Chao (Cornell University Medical College, New York) (Yoon et al., 1996), respectively. Large-scale virus stocks were prepared as described previously (Spector et al., 1998). Stock virus preparations had titers of ~10⁸ pfu/ml and infected the cells with 90% efficiency at a dilution of 1:10. Confluent filter-grown cells (72 h after initial seeding) were infected with adenoviruses (~2 pfu/cell) for 1 h at 37°C. Viruses were diluted in serum-free DME and 300 μl was added to the apical surface, whereas 3 ml of the same medium without virus was added basolaterally. After the virus adsorption phase, media were replaced with serum-containing culture media and the cells were returned to a humidified 5% CO₂ incubator for 36 h before metabolic labeling.

Metabolic Labeling

Filter-grown cells were starved for 30 min at 37°C in DME lacking cysteine and methionine and then radiolabeled for 30 min at 37°C with 0.2 mCi/ml of ³⁵S-Trans label (ICN) diluted in the same medium and added to the basolateral surface (300 μl total volume on a piece of parafilm placed in a tissue culture dish). Medium without radiolabel (1 ml) was added to the apical surface. After this radiolabeling period, cells were washed and incubated at 37°C in DME supplemented with 2 mM cysteine and methionine from 0–150 min. The chase media was collected separately from the apical and basolateral sides at each timepoint to evaluate the secreted protein profiles.

Cell Surface Biotinylation

Confluent filter-grown cells (in some cases metabolically labeled) were washed with ice-cold PBS⁺ and incubated with ice-cold E-Z Link Sulfo-NHS-LC-biotin or E-Z Link Sulfo-NHS-SS-biotin (Pierce) at 0.6 mg/ml prepared in PBS⁺, pH 8.0. Either the apical (1 ml volume) or basolateral (1.5 ml volume) surface was biotinylated twice for 15 min each. The biotinylation reaction was terminated by replacing the second biotin solution with the same volume of ice-cold 50 mM NH₄Cl in PBS for 30 min on ice.

Immunoprecipitations

E-Cadherin. Cells were scraped from the insert in 100 μl of 1% (vol/vol) TX-100, 0.5% (vol/vol) NP-40, 150 mM NaCl, 10 mM Tris-Cl, pH 7.4, 1 mM EDTA, 1 mM EGTA, 0.2 mM sodium vanadate, CLAP (1 μM each of chymostatin, leupeptin, antipain, and pepstatin A), and 1 μM AEBSF. Detergent extracts were incubated with agitation for 1 h at 4°C, after which time insoluble material was removed by centrifugation at 15,000 g for 5 min at room temperature.

LDL-R and p75^{NTR}. Cells were scraped from the insert in 100 μl of 1% (vol/vol) TX-100, 150 mM NaCl, 15 mM Tris-Cl, pH 8.0, 4 mM EDTA, 1 μM CLAP, and 1 μM AEBSF. Detergent extracts were incubated with agitation for 1 h at 4°C, after which time insoluble material was removed by centrifugation at 15,000 g for 5 min at room temperature.

Hemagglutinin. Cells were lysed by addition of 100 μl of SDS lysis buffer (1% [wt/vol] SDS, 15 mM Tris-Cl, pH 8.0, 4 mM EDTA, 1 μM CLAP, and 1 μM AEBSF). The extracts were boiled for 5 min to decrease viscosity of the solution.

All detergent cell extracts were diluted with 900 μl of incubation buffer (0.5% [vol/vol] TX-100, 15 mM Tris-Cl, pH 8.0, 150 mM NaCl, 4 mM EDTA, 1 μM CLAP, 1 μM AEBSF) containing the appropriate dilution of primary antibody. Samples were incubated for 1 h at 4°C with agitation and for an additional 30 min with a rabbit pAb against mouse IgG as a linker antibody when monoclonal primary antibodies were used for immunoprecipitation. Immune complexes were recovered by incubation with 30 μl of protein A-Sepharose (100 μg total IgG binding capacity) (Amersham Pharmacia Biotech) for 1 h at 4°C with agitation. Protein A-Sepharose-bound antibody complexes were recovered after the incubation by centrifugation at 15,000 g for 5 min at room temperature. Immun-

noprecipitates were washed sequentially three times each with 1% (vol/vol) NP-40, 0.1% (wt/vol) SDS, 15 mM Tris-Cl, pH 8.0, 150 mM NaCl, 4 mM EDTA, 1 μ M CLAP, 1 μ M AEBF, with the same buffer except containing 500 mM NaCl, and finally with 50 mM Tris-Cl, pH 8.0. Protein A-Sepharose beads were recovered after each wash by centrifugation at 15,000 *g* for 1 min at room temperature. The beads were resuspended in 50 μ l of 10% (wt/vol) SDS and boiled for 5 min to release the antibody complexes. The supernatant fraction was collected with a narrow-bore pipette tip and 5 μ l was reserved as a measure of the total immunoprecipitated protein, whereas the remainder was diluted in 900 μ l of incubation buffer and reprecipitated with streptavidin-agarose to recover biotinylated proteins as described below.

Streptavidin Affinity Precipitation

Biotinylated samples used to analyze the steady-state distribution of cell surface proteins were solubilized in 100 μ l of SDS lysis buffer. Detergent extracts were boiled for 5 min to denature nucleic acids. The lysate was subsequently diluted in 900 μ l of incubation buffer containing 40 μ l of streptavidin-agarose (sufficient to bind 120 μ g of biotinylated protein) (Pierce), and rocked at 4°C for 1 h. Streptavidin-agarose beads were washed and recovered as described above, and boiled for 5 min in 40 μ l of 2 \times sample buffer (100 mM Tris-Cl, pH 6.8, 4% [wt/vol] SDS, 0.2% [wt/vol] bromophenol blue, 20% [vol/vol] glycerol) containing 50 mM dithiothreitol.

Diluted immunoprecipitates from metabolically labeled samples were incubated with 40 μ l of streptavidin-agarose while rocking at 4°C for 1 h. Streptavidin-agarose beads were washed and recovered as described above, and boiled for 5 min in 40 μ l of 2 \times sample buffer containing 50 mM dithiothreitol.

SDS-PAGE and Immunoblot Analysis

Proteins were separated on 7 or 10% SDS polyacrylamide gels. After electrophoresis, metabolically labeled proteins were detected by drying the gels and subjecting them to phosphorimage analysis with a Fuji PhosphorImager equipped with MacBas software, or a Molecular Dynamics STORM 860 PhosphorImager equipped with ImageQuant software. For immunoblot analyses, proteins resolved by SDS-PAGE were transferred to nitrocellulose membranes (Amersham Pharmacia Biotech). Nonspecific binding sites were blocked by a 1-h incubation at room temperature with 0.5% (wt/vol) nonfat dried milk dissolved in PBS containing 0.1% (vol/vol) Tween-20 (PBS-T). Blots were washed twice for 15 min in PBS-T and incubated with the appropriate dilution of rabbit anti-HA pAb or mouse anti-E-cadherin, anti-rsec6, or anti-rsec8 mAbs for 1 h at room temperature. After two more 15-min washes, blots were probed with the manufacturer's recommended dilution of HRP-conjugated secondary antibody for 30 min at room temperature, washed twice for 5 min with PBS-T, and bound antibodies were detected using chemiluminescent reagents.

Results

ADPKD Cells Form Morphologically Typical and Functionally Intact Tight Junctions

Polarized epithelial cells restrict the paracellular flow of solutes (gate function) and the intermixing of apical and basolateral membrane molecules (fence function) by virtue of their apico-lateral tight junctions (for review see Diamond, 1977). Tight junction integrity was assayed as one measure of the ability of ADPKD cells to establish a polarized cell architecture.

Immunofluorescence microscopy of the tight junction protein occludin (Furuse et al., 1993) was used to examine tight junction morphology. The tight junctions delimited by occludin appeared identical in all patient samples (Fig. 1 A, upper panels). Tight junctions evident by EM consisted of closely apposed membrane contacts, which were morphologically similar in normal kidney and ADPKD cells (Fig. 1 A, lower panels).

Although fluid accumulation within the developing cyst lumen would not be possible without an intact tight junction,

paracellular gate function in explanted ADPKD cells has not been examined previously. ADPKD cells cultured on tissue culture inserts grew in tightly packed monolayers that reached a transepithelial resistance comparable to that of explanted normal kidney epithelial cells (\sim 250 ohms/cm²). This measurement confirmed that the tight junction gate in ADPKD cells was intact.

The integrity of tight junction fence function was ascertained by monitoring the domain-specific localization of the apical membrane protein influenza HA (Matlin et al., 1983). Cell surface HA was detected by membrane domain-specific biotinylation and subsequent immunoblot analysis of streptavidin-precipitated proteins. At steady state, influenza HA was correctly localized on the apical cell membrane of ADPKD cells (Fig. 1 B), indicating that just as in normal kidney cells, diffusion of proteins between membrane domains was prevented. This finding is in agreement with the observation that only select proteins exhibit altered membrane polarity in ADPKD cells in situ (Wilson, 1997). Thus, using these morphological, electrical, and biochemical criteria, ADPKD cells in culture were judged to possess tight junctions indistinguishable from those of their normal kidney counterparts.

ADPKD Cell E-Cadherin Is Not Expressed at the Cell Surface and Is Sequestered in an Intracellular Compartment

The adherens junctions are disposed along the lateral contacting membranes subjacent to the tight junctions, where they play a crucial role in maintaining a polarized epithelium (Drubin and Nelson, 1996). The immunolocalization of the integral membrane protein E-cadherin was examined to assess adherens junction architecture. Polarized monolayers were costained with antibodies against occludin and E-cadherin and imaged by epifluorescence microscopy. The contacting membranes of adjacent normal kidney and ADPKD cells were comparably demarcated by occludin (Fig. 2, upper panels). Normal kidney cell E-cadherin staining (Fig. 2, upper N panel, inset) coincided with that of occludin (Fig. 2, upper N panel) along the lateral cell membranes. Surprisingly, the lateral membranes of ADPKD cells, defined by the disposition of occludin (Fig. 2, upper P panels), were strikingly devoid of E-cadherin (Fig. 2, upper P panels, insets). Because the compartment with which E-cadherin was associated in ADPKD cells was ill-defined by epifluorescence microscopy, the same samples were examined by confocal microscopy to eliminate out-of-focus information (Fig. 2, lower panels). This investigation revealed that whereas E-cadherin was localized solely at the lateral membranes of normal kidney cells (Fig. 2, lower N panel), E-cadherin in ADPKD cells was exclusively sequestered in perinuclear vesicular structures, completely absent from the lateral membranes (Fig. 2, lower P panels). Thus, E-cadherin localization was markedly abnormal in ADPKD cells.

Immunoblot analysis of biotinylated cell surface proteins corroborated the depletion of E-cadherin from the ADPKD cell membrane. E-cadherin was abundant and properly polarized at the basolateral membrane of normal kidney cells (Fig. 3 A, N samples). This contrasted sharply with the absence of any detectable E-cadherin on either the apical or basolateral membrane domains of ADPKD

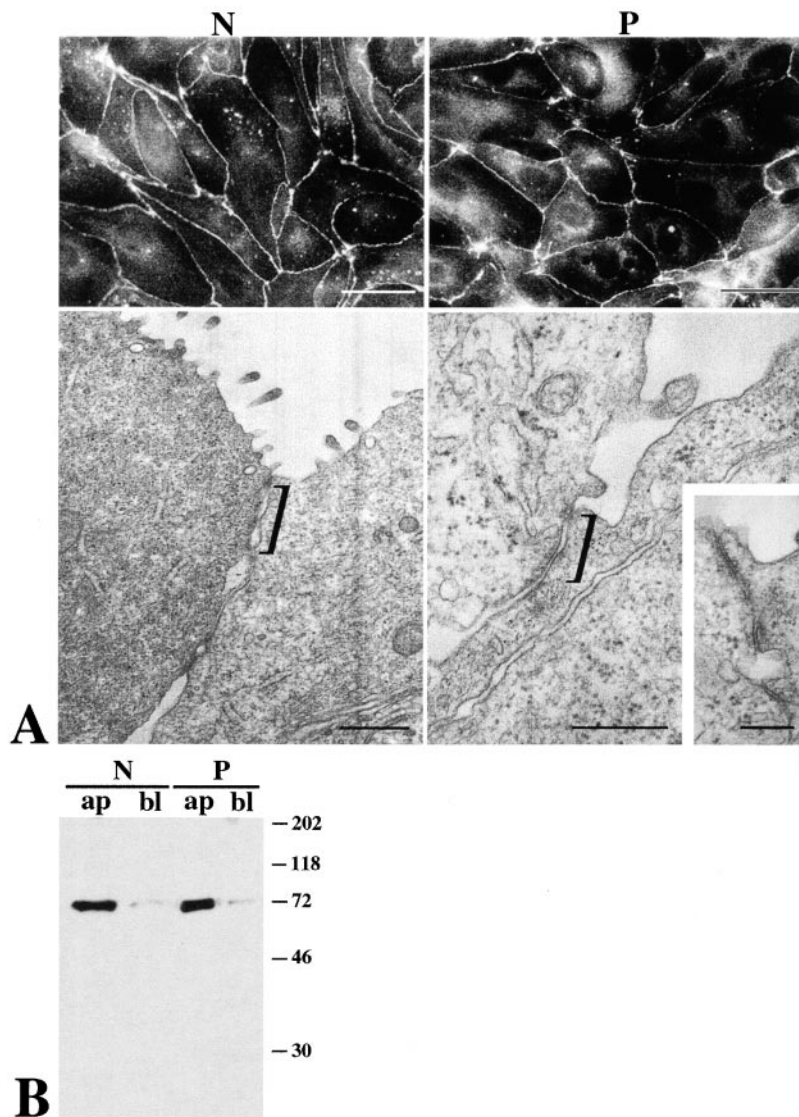


Figure 1. Morphological and functional similarity between normal kidney cell and ADPKD cell tight junctions. (A) Confluent monolayers of normal kidney cells (N) and ADPKD cells (P) on filter inserts were processed for either light or EM. Tight junctions were visualized at the light level by immunostaining with an antibody against occludin followed by an FITC-conjugated secondary antibody. A confocal section collected at the apico-lateral apex is shown (upper panels). The morphology of the tight junction was further examined by electron microscopic analysis of stained and contrasted ultrathin sections (lower panels). Brackets denote tight junctions. Bars: 10 μm (light micrographs); 0.2 μm (electron micrographs); and 0.1 μm (inset). (B) The cell surface polarity of influenza HA in virally infected confluent monolayers of normal kidney cells (N) and ADPKD cells (P) was examined by immunoblot analysis. Filter-grown monolayers were biotinylated at either the apical (ap) or basolateral (bl) surface, cell surface proteins were affinity precipitated with streptavidin-agarose, and the recovered proteins were resolved by SDS-PAGE. Gels were blotted onto nitrocellulose and blots were probed with a rabbit pAb against HA, followed by an HRP-conjugated secondary antibody. HA was detected by the addition of enhanced chemiluminescence substrate and exposure of the blot to X-ray film. The relative migrations of molecular weight standards are as indicated.

cells (Fig. 3 A, P samples). Since ADPKD cells appeared to contain significant amounts of E-cadherin in an intracellular E-cadherin store as judged by confocal analysis (see Fig. 2), the E-cadherin content of cellular extracts was further examined by immunoblot analysis. Three different normal kidney samples expressed similar E-cadherin levels (Fig. 3 B, N samples). In contrast, ADPKD cell patient samples contained lower, variable levels of E-cadherin, although none of the three samples examined lacked the protein entirely (Fig. 3 B, P samples). These results demonstrated that ADPKD cells have reduced levels of E-cadherin, which is improperly sequestered in an intracellular pool. This could be attributed to either decreased synthesis or defective post-Golgi handling, prompting a more detailed analysis of E-cadherin biosynthesis, trafficking, and stability.

Cell Surface Delivery of E-cadherin Is Impaired, while Maturation and Sorting Proceed Efficiently in ADPKD Cells

The absence of E-cadherin at the ADPKD cell membrane raised the possibility that the protein was prevented from

effectively traversing the exocytic pathway. E-cadherin is initially synthesized in association with the ER as a high molecular weight precursor (Peyrieras et al., 1983; Vestweber and Kemler, 1984). Assembly with β -catenin enables transit of E-cadherin to the Golgi apparatus (Chen et al., 1999a), where it is subsequently processed to its mature form (Shore and Nelson, 1991). Information about the molecular maturation, polarized sorting, and cell surface delivery was obtained from metabolic labeling and domain-selective biotinylation experiments. The precursor form of ADPKD cell E-cadherin was synthesized in near-normal amounts and efficiently proteolytically cleaved, demonstrating that ER and Golgi apparatus functions were not generally disrupted in these cells (Fig. 4 A, Total N and P samples). Association of newly synthesized E-cadherin with the catenins was detected by coimmunoprecipitation under the nondenaturing conditions. Multimeric cadherin-catenin complex assembly appeared equally efficient in normal and ADPKD cells (Fig. 4 A, Total basolateral N and P samples). Diminished plasma membrane association of E-cadherin was therefore not due to defective catenin affiliation. However, it was noted that there was a

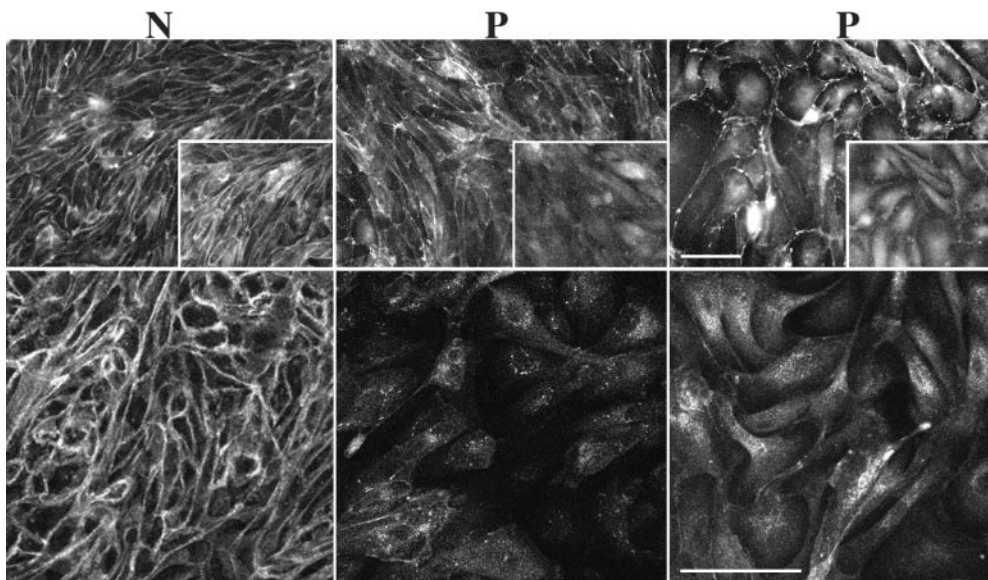


Figure 2. Localization of ADPKD cell E-cadherin to an intracellular compartment. Confluent monolayers of normal kidney cells (N) and ADPKD cells (P) on filter inserts were processed for epifluorescence and confocal microscopy. Junctional complexes were visualized by coimmunostaining the cells with antibodies directed against occludin (rabbit pAb) and E-cadherin (mouse mAb) followed by rhodamine-conjugated anti-rabbit and FITC-conjugated anti-mouse secondary antibodies. The upper panels demonstrate staining of occludin, and the insets in the upper panels depict staining of E-cadherin in the same cells, as viewed by

epifluorescence microscopy. The lower panels portray confocal images of E-cadherin distribution acquired at a single 0.4- μm -thick focal plane along the basolateral membrane. Bars, 10 μm .

significant decrease in E-cadherin delivery to the basolateral surface of ADPKD cells despite near-normal synthesis levels (Fig. 4 A, compare N and P samples in basolateral Cell Surface panel). Importantly, no missorting to the apical membrane was evident at any timepoint (Fig. 4 A, apical Cell Surface panel). Quantification of basolateral delivery showed that at the latest timepoint, only 20% of the protein had arrived at the ADPKD cell surface, compared with 60% in normal kidney cells (Fig. 4 B). Thus, inefficient transport of E-cadherin from the late Golgi cisternae to the plasma membrane is partially responsible for the diminished cell surface-associated E-cadherin observed in ADPKD cells.

Cell Surface Transport of Basolateral Cargo Is Impaired in ADPKD Cells

The polarized sorting and transport of well-characterized apical and basolateral membrane proteins was analyzed to distinguish whether decreased basolateral delivery was unique to E-cadherin or whether a more general defect in vectorial transport existed in ADPKD cells. The cell surface arrival of newly synthesized molecules was scored by metabolic labeling and cell surface biotinylation as described above. Influenza HA was used as an apical marker that is sorted in association with glycosphingolipid rafts (Scheiffele et al., 1997). Within 30 min after pulse labeling, the mature form of influenza HA appeared at the apical cell surface, where it reached maximal levels by 120 min (Fig. 5 A, upper panel). Both the kinetics and amounts of HA delivered to the apical membrane as a percentage of total newly synthesized HA were similar in normal kidney and ADPKD cells (Fig. 5 B). Delivery of HA to the basolateral membrane was undetectable in both normal and ADPKD cells (Fig. 5 A, lower panel).

Neurotrophin receptor (p75^{NTR}) served as a second apical marker that is sorted by virtue of its luminal O-linked

glycosylation (Yeaman et al., 1997). As was observed for influenza HA, p75^{NTR} delivery to the apical membrane of ADPKD cells was identical to that documented in normal kidney cells (Fig. 5 C). Approximately 30% of the total ³⁵S-labeled p75^{NTR} was scored as having reached the cell surface during the chase period by biotinylation. Similar amounts of p75^{NTR} were seen delivered to the surface of MDCK cells in an analogous experiment, where it was determined that this was an under-representation of cell surface delivery most likely due to inefficient biotinylation and/or streptavidin recovery (Grindstaff et al., 1998).

Complementary experiments were conducted to examine the cell surface delivery of the basolaterally targeted LDL-R, the sorting signal for which resides in the cytoplasmic domain (Matter et al., 1992). In normal kidney cells, LDL-R was first detected at the cell surface within 30 min after pulse labeling and increased steadily over the course of the 120-min chase period (Fig. 6 A, Cell Surface samples, N lanes). The synthesis of LDL-R and processing of the precursor to the mature form proceeded with comparable kinetics in ADPKD cells and normal kidney cells (Fig. 6 A, Total samples, compare N and P lanes). However, the rate of LDL-R cell surface delivery was diminished twofold in ADPKD as compared with normal kidney cells (Fig. 6 B). Missorting of LDL-R to the apical membrane domain was not evident (Fig. 6 C). In two of the three ADPKD patient samples analyzed, the mobility of the mature form of LDL-R during SDS-PAGE was slightly faster than LDL-R from normal kidney cell samples (Fig. 6 A and data not shown), likely indicative of minor differences in posttranslational processing. Since basolateral transport efficiency was similarly diminished in all three samples and in no case was there any impact on polarized LDL-R sorting, it is felt that processing differences are inconsequential with respect to the trafficking deficit. Instead, the reduced efficiency of basolateral LDL-R delivery was reminiscent of the impaired transport of nor-

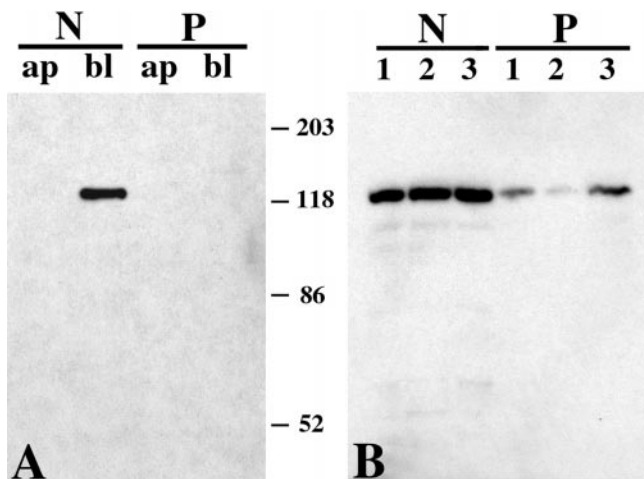


Figure 3. Absence of ADPKD cell E-cadherin at the cell surface and diminished E-cadherin expression. (A) The cell surface polarity of E-cadherin in confluent monolayers of normal kidney cells (N) and ADPKD cells (P) was examined by immunoblot analysis. Filter-grown monolayers were biotinylated at either the apical (ap) or basolateral (bl) surface, cell surface proteins affinity precipitated with streptavidin-agarose, and recovered proteins resolved by SDS-PAGE. Gels were blotted onto nitrocellulose and the blots were probed with a mouse mAb against E-cadherin followed by an HRP-conjugated secondary antibody. E-cadherin was detected by the addition of enhanced chemiluminescence substrate and exposure of the blot to X-ray film. (B) Expression levels of total cellular E-cadherin were examined by immunoblot analysis of extracts from three patient samples of normal kidney cells (N, lanes 1, 2, and 3) and ADPKD cells (P, lanes 1, 2, and 3). Proteins in the detergent extracts (10 μ g/lane) were resolved by SDS-PAGE. E-cadherin was detected by immunoblot analysis as described in A. The relative migration of molecular weight standards are as indicated.

mally assembled and processed E-cadherin to the ADPKD basolateral surface.

Polarized secretion of newly synthesized proteins was examined as a further measure of overall protein trafficking to the apical and basolateral plasma membrane domains. This was accomplished by collecting the media separately from the apical and basolateral chambers of metabolically labeled, filter-grown cells. Comparisons of the secreted protein profiles after SDS-PAGE and autoradiography demonstrated that most apical proteins were secreted with identical kinetics in comparable amounts in both cell types up to the 60 min timepoint (Fig. 7 A). It was noted that apical proteins secreted by ADPKD cells failed to increase in amounts beyond those present at the 60 min timepoint, which may represent either enhanced protein degradation on account of enhanced internalization or elevated protease activity by polycystic kidney disease cells (Rankin et al., 1996). In marked contrast to apical protein secretion, comparisons of basolateral protein secretion revealed a disparity in the efficiency of basolateral exocytosis at all timepoints (Fig. 7 B). Normal kidney cells steadily secreted increasing amounts of several proteins into the basolateral medium (Fig. 7 B, arrowheads). Basolateral secretion from ADPKD cells was significantly reduced, with very little secreted protein detectable even at the latest timepoint (Fig. 7 B, P lanes), in keeping with the observations made in the analyses of individual baso-

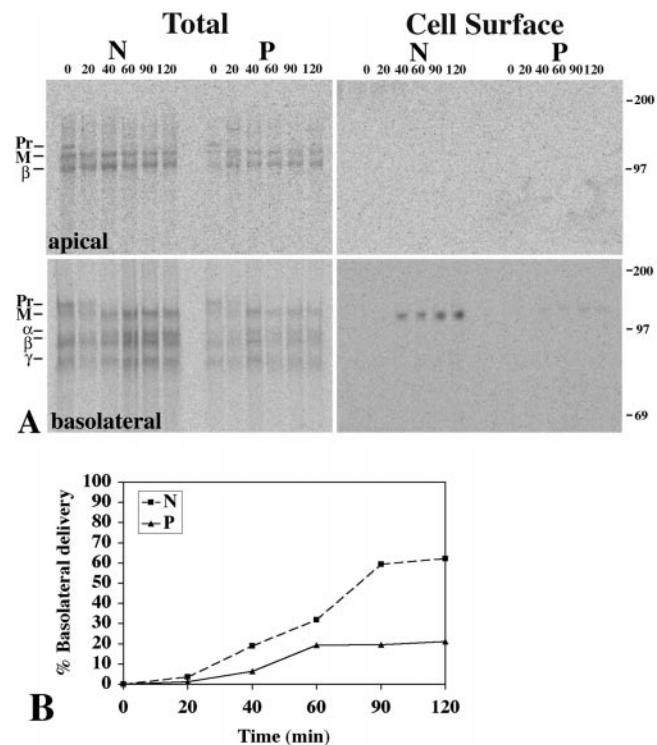


Figure 4. Inefficient basolateral delivery of ADPKD cell E-cadherin. Filter-grown monolayers of normal kidney cells (N) and ADPKD cells (P) were metabolically labeled with 35 S-Trans label and incubated for the indicated chase periods to allow newly synthesized proteins to reach the cell surface. At each timepoint, proteins on either the apical or basolateral membrane were biotinylated, nondenaturing cellular extracts were prepared, and E-cadherin immunoprecipitated with a mouse mAb against E-cadherin. 10% of the recovered protein was reserved as a measure of total newly synthesized cellular E-cadherin (Total), whereas the biotinylated proteins in the remaining immunoprecipitate were affinity-precipitated with streptavidin-agarose (Cell Surface). (A) Proteins were separated by SDS-PAGE, and dried gels subjected to phosphorimage analysis. α , β , and γ denote the catenins coimmunoprecipitated with E-cadherin. M, mature form of E-cadherin; Pr, E-cadherin precursor. The relative migration of molecular weight standards are as indicated. (B) The amount of radioactive E-cadherin delivered to the basolateral membrane as a percent of total newly synthesized E-cadherin (shown in A, lower Cell Surface panel) was quantified by phosphorimage analysis. Data from a representative experiment are shown.

lateral membrane proteins. Based on this series of experiments, it was apparent that protein transport to the basolateral cell surface was impaired, whereas apical delivery proceeded relatively unimpeded.

Exocytic Cargo Is Retained in the ADPKD Cell Golgi Apparatus

Diminished cell surface delivery of newly synthesized basolateral cargo in the absence of any posttranslational processing deficits or apical mistargeting prompted an investigation of whether molecules might be accumulating in the ADPKD cell Golgi apparatus. To explore this possibility, the fluorescent lipid analogue C₆-NBD-ceramide was used to assay Golgi-to-plasma membrane transport both mor-

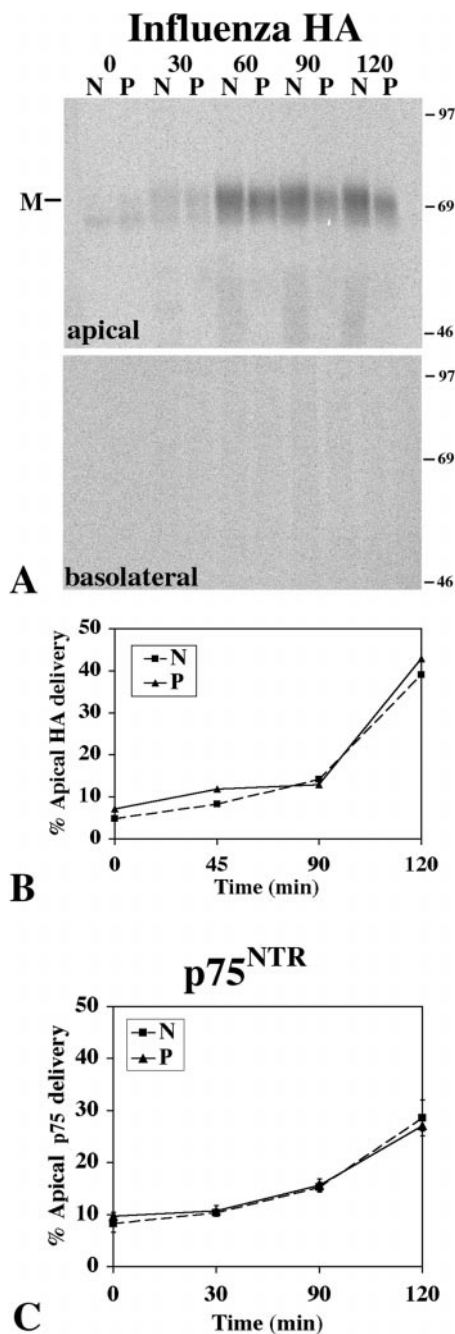


Figure 5. Polarized delivery of two apical membrane proteins to the surface of ADPKD cells proceeds normally. (A) Filter-grown cells were infected with influenza virus and metabolically labeled as detailed in Materials and Methods. Cell surface delivery of influenza HA was scored by domain-selective biotinylation after the indicated chase periods. The biotinylated HA was recovered by sequential immunoprecipitation and streptavidin precipitation, resolved by SDS-PAGE, and visualized by phosphorimage analysis. The upper panel depicts influenza HA recovered from cells biotinylated on the apical cell surface. The lower panel shows the extent of biotinylated influenza HA recovered when cells were biotinylated at the basolateral surface. (B) The amount of radioactive HA delivered to the apical membrane as a percent of total newly synthesized HA was quantified by phosphorimage analysis. Averaged values from two such experiments are shown. (C) Filter-grown cells were infected with recombinant adenovirus expressing p75^{NTR}, metabolically labeled, and apical cell sur-

face delivery of p75^{NTR} was scored as described in A. The results of all three experimental trials were quantified. The mean values \pm SD are plotted. M, mature influenza HA; N, normal kidney cells; and P, ADPKD cells.

phologically and biochemically as described (Lipsky and Pagano, 1985; van Meer et al., 1987). Cellular membranes were labeled with C₆-NBD-ceramide at reduced temperature (20°C) for 90 min, after which time cell surface C₆-NBD-ceramide was removed by back-exchange at low temperature. Under these conditions, C₆-NBD-ceramide was delivered to the Golgi apparatus, where it was similarly metabolized to C₆-NBD-glucosylceramide and C₆-NBD-sphingomyelin in both normal kidney and ADPKD cells (data not shown). The inhibition of vesicular transport to the cell surface caused by the 20°C incubation resulted in the accumulation of these fluorescent lipid metabolites in the TGN of both normal and ADPKD cells (Fig. 8, 0 min). Golgi-to-cell surface transport of the C₆-NBD-lipids was initiated by transferring the cells to 37°C and cell surface delivery was monitored by confocal microscopy (Fig. 8, 30–90 min). These experiments revealed a dramatic defect in the ability of ADPKD cells to transport the C₆-NBD-lipids to the cell surface (Fig. 8, compare P samples with N samples). In normal kidney cells, the C₆-NBD-lipids were first evident at the basolateral plasma membrane within 30 min after warming to 37°C, and cell surface delivery was complete by 90 min, with none remaining Golgi-associated at the latter timepoint. In contrast, basolateral delivery in ADPKD cells was not detectable after 90 min, and the C₆-NBD-lipids remained associated with the ADPKD cell Golgi apparatus for as long as 150 min (Fig. 8, P 90 min sample; data not shown). Quantitative analyses of cell surface fluorescent lipids extracted from the apical or basolateral membrane domains indicated that lipid transport to the ADPKD cell basolateral membrane was reduced by 2.5–3-fold, whereas apical delivery was unimpeded (data not shown).

Components of the Basolateral Targeting Patch Are Depleted from the ADPKD Cell Membrane

The demonstration that C₆-NBD-lipids failed to exit the Golgi apparatus, coupled with the observed basolateral trafficking defect, were indicative of defective vectorial trafficking from the ADPKD cell Golgi apparatus to the basolateral plasma membrane. Ineffective delivery of exocytic cargo to the ADPKD cell basolateral membrane raised the possibility that constituents of the basolateral targeting patch were improperly expressed or localized. The localization of sec6 and sec8 was therefore examined by confocal microscopy. Cells were stained to visualize sec6 or sec8 (red channel) in parallel with the tight junction protein occludin (green channel). In normal kidney cells, both sec6 and sec8 were localized in close apposition to the tight junction protein occludin (Fig. 9 A, left panels). In contrast, both proteins were depleted from the ADPKD cell lateral membranes and appeared diffusely dispersed throughout the cytoplasm (Fig. 9 A, right panels). Immunoblot analyses revealed that sec6 and sec8 protein levels were similar in all normal kidney and ADPKD samples analyzed (Fig. 9 B, compare N and P samples).

face delivery of p75^{NTR} was scored as described in A. The results of all three experimental trials were quantified. The mean values \pm SD are plotted. M, mature influenza HA; N, normal kidney cells; and P, ADPKD cells.

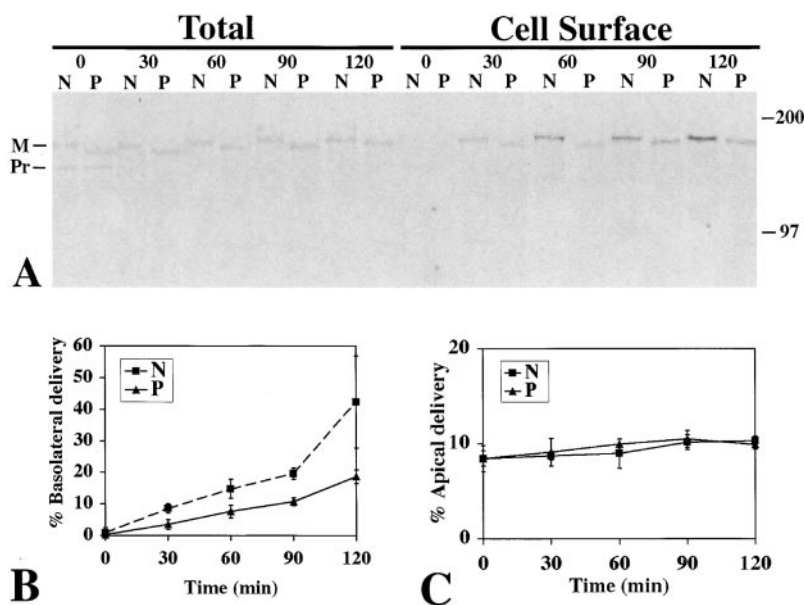


Figure 6. Basolateral membrane protein transport to the cell surface is impaired in ADPKD cells. Filter-grown cells were infected with recombinant adenovirus expressing LDL-R and metabolically labeled as detailed in Materials and Methods. Cell surface delivery of LDL-R was scored by domain-selective biotinylation after the indicated chase periods. Radiolabeled LDL-R was recovered by immunoprecipitation (Total samples) and the biotinylated fraction was subsequently recovered by streptavidin precipitation (Cell Surface samples). All samples were resolved by SDS-PAGE and visualized by phosphorimage analysis. (A) Total samples represent one-tenth of the total immunoprecipitated LDL-R, whereas Cell Surface samples represent the basolaterally biotinylated LDL-R recovered from the remainder of the immunoprecipitates. A typical result from three separate trials, each performed with one of three different normal and one of three different ADPKD cell samples, is shown. M, mature form of LDL-R; Pr, ER precursor form of LDL-R; N, normal kidney cells; and P, ADPKD cells. (B and C) The results of all three trials were quantified. The mean values \pm SD are plotted. (B) Quantification of basolateral cell surface appearance of LDL-R. (C) Quantification of apical cell surface appearance of LDL-R.

Therefore, sec protein redistribution was not accompanied by a decline in sec protein expression, as was observed for E-cadherin. These results substantiate a marked disruption in the integrity of the basolateral cargo delivery site in ADPKD cells, likely brought about by altered E-cadherin-based adherens junction assembly.

Discussion

This study identified the loss of cell surface E-cadherin and the exocyst components sec6 and sec8 as critical molecular deficits affecting ADPKD epithelial cells. Although ADPKD cells possessed characteristics of polarized cells, the disease cells suffered from a lack of detectable cell surface E-cadherin. Total cellular E-cadherin levels were lower than those in normal kidney cells, and existing E-cadherin was sequestered in an intracellular pool. The cell surface depletion of sec6 and sec8 in ADPKD cells devoid of plasma membrane-associated E-cadherin was correlated with significantly impaired delivery of proteins and lipids to the basolateral cell surface. Vectorial transport to the apical ADPKD cell surface, on the other hand, was functionally intact. Together, the investigations presented here serve to clarify the molecular mechanisms whereby mutations in PKD1 or PKD2 may lead to downstream alterations in cytoarchitecture and molecular trafficking in ADPKD cells.

E-cadherin, the catenins, and the polycystins are all disposed within the basolateral membrane beneath the apicolateral tight junction, where recent data suggest they are engaged in a large multimeric complex that may coordinately regulate cellular organization (Fig. 10) (Ibraghimov-Beskrovnyaya et al., 1997; Obermüller et al., 1999; Wu et al., 1998; Yeaman et al., 1999). E-cadherin, as the trans-

membrane component of adherens junctions, constitutes the calcium-dependent molecular link between adjacent cell membranes that implements cytoskeletal organization via cytosolic catenins (Drubin and Nelson, 1996). Association of polycystin-1 with the E-cadherin-catenin assembly (Huan and van Adelsberg, 1999) is expected to tether a subset of polycystin-1 molecules in close proximity to adherens junctions. Polycystin-1, with its numerous cell-cell and cell-extracellular matrix adhesion domains, is thus poised to facilitate interactions with neighboring cells or the matrix. Demonstrated interactions between polycystin-2 and polycystin-1 (Tsiokas et al., 1997) merit the inclusion of polycystin-2 within this complex. Given the likelihood of an ordered assembly between adherens junction components and the polycystins, it is interesting to consider why E-cadherin and sec6/8 might be depleted from the cell surface of ADPKD cells, and what ramifications this may have on cellular organization.

Mechanisms Underlying Loss of Cell Surface E-Cadherin

It is plausible that the physical association of E-cadherin with mutant polycystin-1 might lead to the disruption of epithelial cell organization, particularly given the demonstrated interaction between polycystin-1 and E-cadherin (Huan and van Adelsberg, 1999). The developmental downregulation of polycystin-1 expression is altered in ADPKD so that mutant PKD1 products are often overexpressed (Geng et al., 1996, 1997). Conceivably, overexpressed mutant polycystin-1 may adversely impact E-cadherin stability. Indeed, the patient-to-patient variability in E-cadherin expression levels in ADPKD cells demonstrated here indicates that individual polycystin mutations

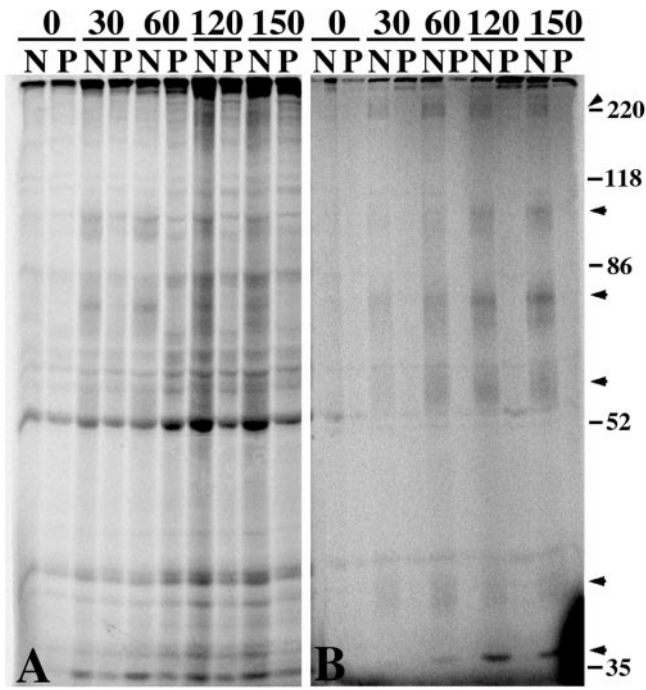


Figure 7. ADPKD cells exhibit defective basolateral secretion. Filter-grown cells were metabolically labeled for 30 min and culture media were collected from the apical or basolateral filter chamber after various periods of chase (0–150 min). Metabolically labeled proteins secreted into the (A) apical or (B) basolateral medium were resolved by SDS-PAGE and detected by autoradiography. N, normal kidney cells; and P, ADPKD cells. Arrowheads denote basolateral secreted proteins.

differentially influence E-cadherin stability. Disturbances in either the stoichiometry of normal E-cadherin–polycystin-1 interactions or the structural characteristics of such complexes could account for the compromised efficiency with which E-cadherin is transported through the late exocytic pathway and stably retained at the plasma membrane in multiple ways. This report demonstrated that *de novo* membrane insertion, plasma membrane stabilization, and recycling or degradation of E-cadherin are all affected in ADPKD cells. Diminished E-cadherin cell surface delivery undoubtedly contributes to the reduced cell surface expression, although given the threefold decrease in delivery, this deficit cannot entirely account for the lack of ADPKD cell surface E-cadherin observed at steady state. E-cadherin was recently demonstrated to undergo dynamic recycling between the cell surface and early endosomes, traversing a circuit through which the plasma membrane disposition of E-cadherin may be regulated (Le et al., 1999). In light of this finding, it is interesting to consider that modulation of a regulatory circuit may contribute to reduced cell surface expression of E-cadherin in ADPKD cells. Aberrant assembly of multimeric E-cadherin-containing complexes may cause the newly synthesized E-cadherin arriving at the basolateral cell surface to be increasingly internalized and decreasingly recycled to the plasma membrane, resulting in the observed intracellular accumulation. The existence of a pathogenic variation in this circuit is further suggested by the diminished levels of E-cad-

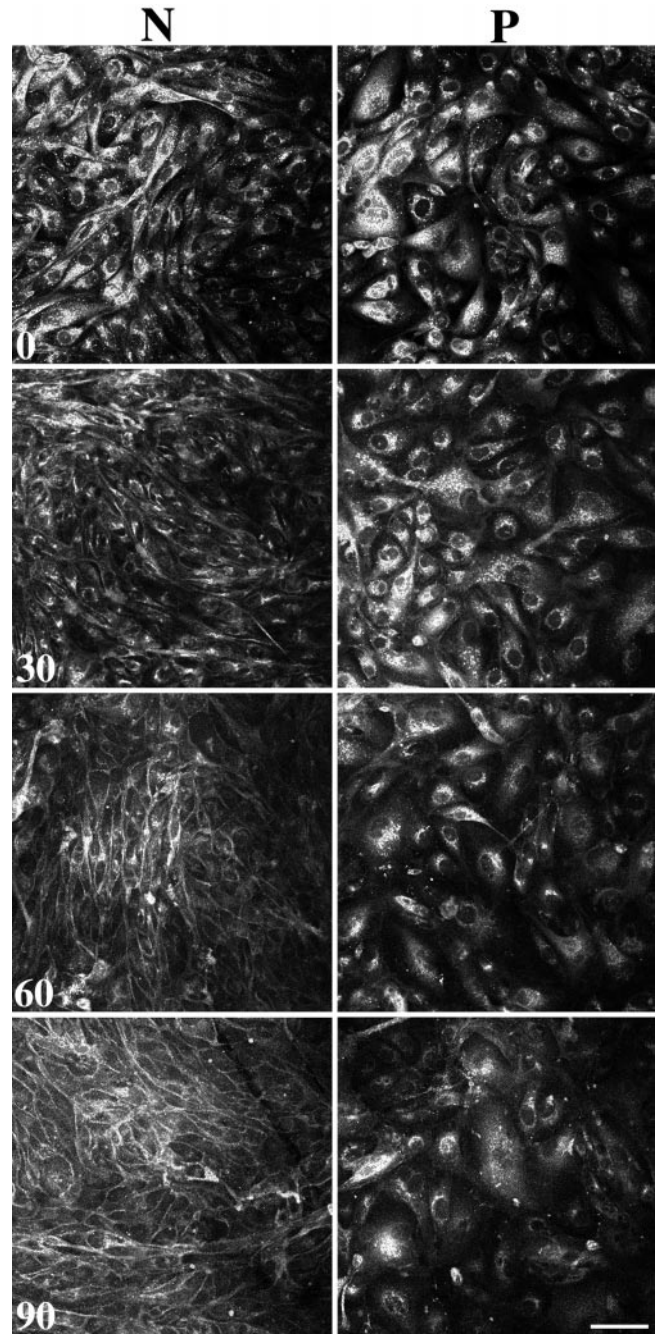


Figure 8. Fluorescent lipids fail to reach the ADPKD cell surface. Filter-grown cells were labeled with C_6 -NBD-ceramide at 20°C and its C_6 -NBD lipid metabolites were allowed to accumulate in the TGN (time 0 samples). Subsequently, the cells were warmed to 37°C for the indicated times (30–90 min) to allow the synchronous transport of C_6 -NBD lipids from the Golgi to the plasma membrane. Each image depicts a single 0.4- μ m confocal section acquired at the basolateral cell surface. N, normal kidney cells; and P, ADPKD cells. Bar, 10 μ m.

herin in ADPKD cells: once internalized, unrecycled abnormal E-cadherin complexes may be transported to late endocytic organelles and degraded. Depletion of the exocyst complex from the basolateral membrane upon the acquisition of a second, somatic genetic lesion is likely a

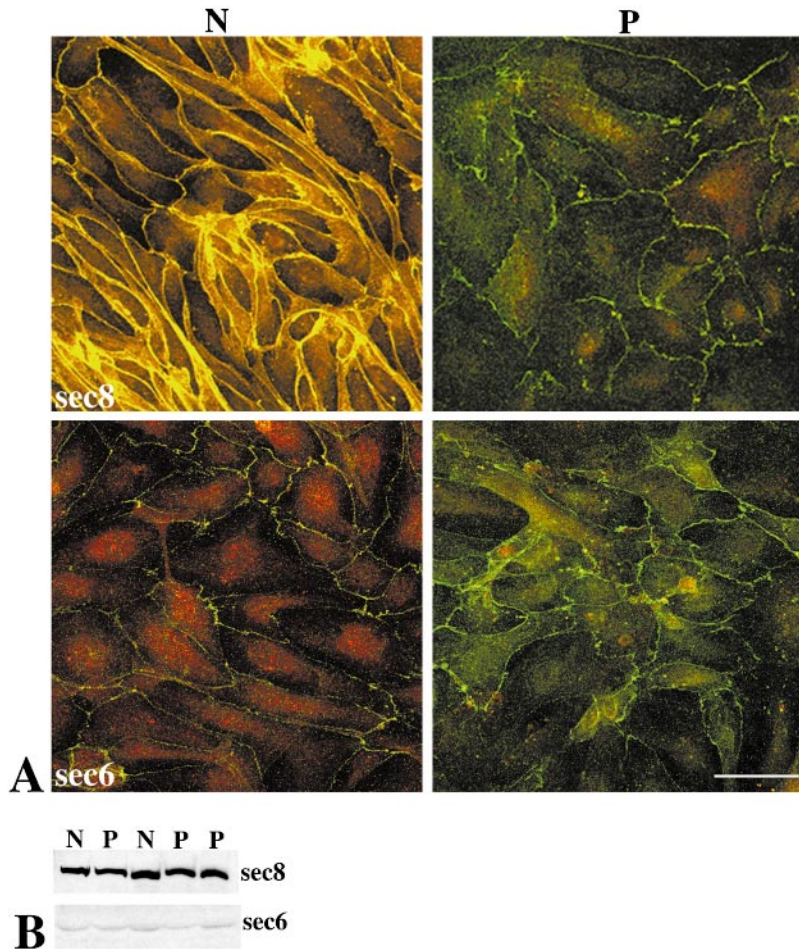


Figure 9. Depletion of sec8 and sec6 from the ADPKD cell membrane without loss of expression. (A) Confluent monolayers of normal kidney cells (N) and ADPKD cells (P) on filter inserts were processed for confocal microscopy. The association of sec8 and sec6 with the apico-lateral membrane region was assessed by coimmunostaining the cells with a rabbit pAb against occludin and mouse mAbs against either sec8 or sec6, followed by FITC-conjugated anti-rabbit and rhodamine-conjugated anti-mouse secondary antibodies. Confocal images (0.4- μ m-thick focal sections) were collected along the entire height of the cells and assembled as an extended focus image of 50 such focal sections. Occludin staining appears green, whereas sec8 or sec6 staining appears red. Colocalization of occludin with either sec8 or sec6 is evident by a yellow overlap pattern. Bar, 10 μ m. (B) Expression levels of sec8 and sec6 were examined by immunoblot analysis of total cellular proteins from filter-grown monolayers of two patient samples of normal kidney cells (N) and three patient samples of ADPKD cells (P). Proteins in detergent extracts (10 μ g/lane) were resolved by SDS-PAGE. Gels were blotted onto nitrocellulose and blots were probed with mouse mAbs against sec8 or sec6, followed by an HRP-conjugated secondary antibody. sec8 and sec6 were detected by the addition of enhanced chemiluminescence substrate and exposure of the blot to X-ray film.

downstream event that follows a reduction in cell surface E-cadherin. Dissociation of the basolateral cargo targeting patch from the apico-lateral apex may exacerbate the defect by precluding further delivery of newly synthesized E-cadherin, and by impacting recycling of E-cadherin to the basolateral membrane. Although future studies are needed to clarify the precise mechanisms by which mutations in PKD1 or PKD2 affect E-cadherin trafficking and stability, it is probable that deranged intermolecular interactions involving E-cadherin constitute potent stimuli culminating in cellular dysmorphogenesis in ADPKD.

Cell-Cell Adhesion in the Absence of Cell Surface E-Cadherin

E-cadherin has been suggested to occupy a central role in the nucleation and maintenance of epithelial cell polarity (Drubin and Nelson, 1996). When E-cadherin ligation was prevented, both adherens junction as well as tight junction and desmosomal junction assembly were inhibited (Gumbiner et al., 1988). Nevertheless, in the absence of detectable cell surface E-cadherin, explanted ADPKD cells are somehow capable of maintaining partially polarized, physically intact monolayers. The possibility that alternate cadherins are present on the ADPKD cell surface, sufficing to generate a partially polarized phenotype, was explored by immunochemical analyses of K-cadherin and the cadherins in general. K-cadherin/cadherin-6 is a cadherin fam-

ily member expressed during renal development as well as in mature proximal tubule cells (Xiang et al., 1994; Shimoyama et al., 1995; Paul et al., 1997). K-cadherin protein levels in both normal and ADPKD cells were low, and no compensatory changes were evident (data not shown). However, immunostaining using a pan-cadherin antibody directed against a highly conserved region shared by cadherin proteins demonstrated that the lateral membranes of ADPKD cells contained an alternate cadherin (data not shown). Thus, adhesion through an alternate cadherin family member, in concert with integrin- and desmosome-mediated adhesion, may compensate for the loss of cell surface E-cadherin and serve to support ADPKD cell architecture.

Mechanisms Underlying Altered ADPKD Cell Polarity

The nonpolarized distribution of certain basolateral membrane proteins in ADPKD cyst-lining cells led to the tenable hypothesis that polarized trafficking is defective (Wilson, 1997), which has until now remained untested. Quite unexpectedly, even in the absence of efficient basolateral delivery, E-cadherin and LDL-R were not mistargeted to the apical ADPKD cell membrane. These findings exclude promiscuous packaging of exocytic cargo within the TGN and aberrant targeting of basolateral vesicles as contributing factors in abnormal ADPKD cell polarity. Therefore, it is necessary to consider alternative explanations for

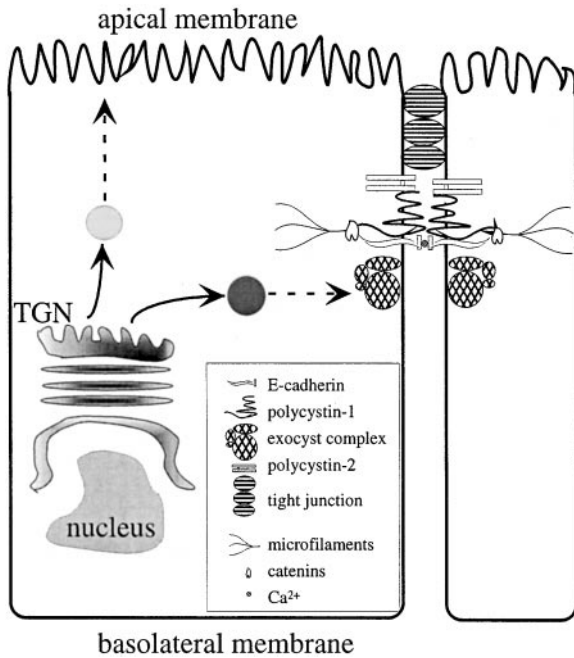


Figure 10. A multimeric complex involved in epithelial cell organization. The diagram depicts current knowledge regarding the localizations of the polycystins, adherens junction proteins, and exocyst components. A legend identifies each component and detailed functional descriptions are given in the text. Polycystin-1 is depicted in contact with E-cadherin and catenins, though it is not known whether the association is direct or involves intermediary proteins.

immunohistochemical (Wilson, 1997) and pharmacological (Du and Wilson, 1995; Wilson et al., 1991) evidence that ADPKD cells are not fully polarized. Typically, a minor fraction of newly synthesized plasma membrane proteins escape sorting within the TGN of normal kidney epithelial cells, and as a result, are delivered to the incorrect membrane (Simons and Fuller, 1985). These molecules are subsequently internalized and redirected along the endocytic/transcytotic pathway to the correct plasma membrane domain. Upon arrival at the basolateral plasma membrane, proteins such as the Na⁺, K⁺ adenosine triphosphatase (Na⁺, K⁺-ATPase) become stably linked to microfilament assemblies, the organization of which depends on proper E-cadherin ligation (Yeaman et al., 1999). The loss of cell surface E-cadherin expression observed here is thus most likely the key to understanding deficits in ADPKD cell polarity. Given the disturbances in ADPKD cell architecture observed *in situ* (Wilson et al., 1986) coupled with the alterations in E-cadherin localization demonstrated in cultured ADPKD cells, it seems plausible that the small fraction of basolateral molecules initially mistargeted to the apical membrane (below detection levels in the cell surface delivery experiments) become stabilized within the incorrect membrane. Inappropriate apical membrane localization might occur through aberrant cytoskeletal interactions, or alternatively because endocytosis/transcytosis processes critical for retrieving mistargeted molecules to the correct membrane domain are dysfunctional. It is also possible that missorting in ADPKD is con-

ditioned to select membrane proteins due to specialized, as-yet undefined transport requirements. Any of these possible mechanisms would facilitate the accumulation of basolateral cargo at the incorrect membrane domain and may account for the stable, functionally active Na⁺, K⁺-ATPase and EGF receptor at the incorrect (luminal/apical) surface in ADPKD cysts (Wilson et al., 1991; Du and Wilson, 1995). Given the dramatic reorganization of ADPKD epithelial cells described in this study, it will now be of great interest to determine how the modulations in E-cadherin and sec6/8 localization contribute to the defects in ADPKD cell membrane polarity.

Inefficient ADPKD Cell Trafficking: Stalling of TGN-to-Basolateral Membrane Transport

Once the TGN processes of sorting and vesicle formation are complete, basolateral cargo is generally transported directly to the cell surface of kidney epithelial cells, although a subset may pass through endosomes (Lisanti et al., 1989; Le Bivic et al., 1990; Futter et al., 1995; Leitinger et al., 1995). The experiments described in this study have spatially placed the basolateral trafficking deficit in ADPKD cells between vesicle formation at the TGN and fusion with the plasma membrane.

Generalized alterations in ER-to-Golgi transport were excluded as a cause for the basolateral membrane trafficking defect in ADPKD cells by monitoring the processing of several exocytic transport markers. Posttranslational modification of apical (influenza HA) as well as basolateral (LDL-R and E-cadherin) cargo proceeded at the same rate in ADPKD and normal kidney cells. Delays in multimeric assembly of E-cadherin–catenin complexes were also not observed. Furthermore, lipid metabolism, measured as the conversion of C₆-NBD-ceramide into C₆-NBD-glucosylceramide and C₆-NBD-sphingomyelin within the Golgi apparatus, occurred with similar kinetics in ADPKD and normal kidney cells (data not shown). The finding that these processes were largely unaffected pinpointed the exocytic defect to a late basolateral trafficking event.

After polarized molecular sorting in the ADPKD cell Golgi apparatus, basolateral trafficking is arrested, with basolateral cargo failing to exit this organelle. Morphological evidence that export of molecules from the ADPKD cell Golgi apparatus was impeded was furnished by experiments tracing the transport of fluorescent lipids. Ineffective transport was evident by the retention of C₆-NBD lipids within the ADPKD cell Golgi apparatus long after those in normal kidney cells had traversed the Golgi apparatus and been efficiently delivered to the basolateral membrane. Impaired export from the ADPKD cell Golgi apparatus was also apparent from the delayed protein transport to the basolateral cell surface. Since ER-to-Golgi transport was unimpaired and there was no evidence of apical mistargeting, this implied that analogous to the lipid markers, basolateral proteins were detained within the Golgi apparatus. Evaluations of ADPKD cell Golgi apparatus morphology documented conspicuously dilated cisternae (Charron, A.J., R.L. Bacallao, and A. Wandering-Ness, manuscript in preparation), which may be readily explained by the aberrant retention of basolat-

erally destined molecules within the Golgi apparatus. Impediment of cargo export from the Golgi apparatus may be indicative of regulatory mechanisms coordinating vesicle budding and vesicular fusion with the target (basolateral) ADPKD cell membrane.

Docking and fusion of vesicles with the plasma membrane embodies the ultimate step in basolateral trafficking. This step is mediated by the concerted actions of the SNARE proteins and exocyst components (Chen et al., 1999b; Grindstaff et al., 1998). Examination of SNARE protein distribution using antiserum against the basolateral SNARE protein syntaxin 4 did not reveal noticeable differences in its distribution between the two cell types (Charron, A.J., R.L. Bacallao, and A. Wandinger-Ness, manuscript in preparation). This component of the basal docking and fusion machinery is therefore likely intact, and may partially compensate for the depletion of the basolateral targeting patch from the ADPKD cell membrane, mediating residual basolateral transport. However, the loss of sec6 and sec8 from the ADPKD cell membrane presumably impacts not only the final event in basolateral exocytosis, but also cellular organization per se. Given the central role of E-cadherin in maintaining epithelial cell organization, impaired docking and fusion of plasma membrane-bound E-cadherin-containing vesicles due to dissociation of sec6/8 from the basolateral targeting patch likely directly impacts cytoarchitecture, as discussed above. In addition, it is also conceivable that the dispersal of exocyst components affects the exocytic organelles. Basolateral cargo-bearing vesicles that leave the ADPKD cell Golgi apparatus and are transported to the membrane region normally associated with the exocyst complex may become stalled, as efficient docking and fusion is prevented. By engaging basolateral trafficking effectors in futile post-Golgi transport, this effect is expected to eventually lead to diminished basolateral vesicle budding from the ADPKD cell Golgi apparatus. If such a retrograde pathogenic mechanism issuing from the cell surface back to the Golgi exists, it is reasonable to postulate that the acquisition of mutations in the PKD1 or PKD2 loci would set into motion a cascade of events, commencing with the destabilization of cell surface E-cadherin and ultimately culminating in the ADPKD epithelial cell phenotype.

We pay special tribute to the memory of Dr. Frank Carone, a friend and collaborator whose unflinching determination and pioneering spirit remain as a constant source of inspiration to all of us. We gratefully acknowledge Ms. Janice Pennington for electron microscopic imaging. Ms. Mary Slater and Ms. Elsa Romero provided valuable assistance with general laboratory management.

This work was supported by grants from the National Institute of Diabetes and Digestive and Kidney Diseases to A. Wandinger-Ness (R01 DK 50141) and R. Bacallao (R29 DK 46883). R. Bacallao is also a recipient of a Clinician Scientist Award from the National Kidney Foundation. A.J. Charron was partially supported by a National Institute of General Medical Sciences predoctoral training grant (T32 GM 08061).

Submitted: 29 September 1999

Revised: 21 February 2000

Accepted: 23 February 2000

References

Carone, F.A., S. Nakaumura, B.S. Schumacher, P. Punyari, and X. Bauer. 1989. Cyst-derived cells do not exhibit accelerated growth or features of

- transformed cells in vitro. *Kidney Int.* 35:1351-1357.
- Carone, F.A., R. Bacallao, and Y.S. Kanwar. 1994. Biology of polycystic kidney disease. *Lab. Invest.* 70:437-448.
- Chen, Y., D.B. Stewart, and W.J. Nelson. 1999a. Coupling assembly of the E-cadherin/beta catenin complex to efficient endoplasmic reticulum exit and basal-lateral membrane targeting of E-cadherin in polarized MDCK cells. *J. Cell Biol.* 144:687-699.
- Chen, Y.A., S.J. Scales, S.M. Patel, Y. Doung, and R.H. Scheller. 1999b. SNARE complex formation is triggered by Ca^{2+} and drives membrane fusion. *Cell.* 97:165-174.
- Daoust, M.C., D.G. Reynolds, D.G. Bichet, and S. Somlo. 1995. Evidence for a third genetic locus for autosomal dominant polycystic kidney disease. *Genomics.* 25:733-736.
- Diamond, J.M. 1977. Twenty-first Bowditch lecture. The epithelial junction: bridge, gate, and fence. *Physiologist.* 20:10-18.
- Drubin, D.G., and W.J. Nelson. 1996. Origins of cell polarity. *Cell.* 84:335-344.
- Du, J., and P. Wilson. 1995. Abnormal polarization of EGF receptors and autocrine stimulation of cyst epithelial growth in human ADPKD. *Am. J. Physiol.* 269:C487-C495.
- Furuse, M., T. Hirase, M. Itoh, A. Nagafuchi, S. Yonemura, S. Tsukita, and S. Tsukita. 1993. Occludin: a novel integral membrane protein localizing at tight junctions. *J. Cell Biol.* 123:1777-1788.
- Futter, C.E., C.N. Connolly, D.F. Cutler, and C.R. Hopkins. 1995. Newly synthesized transferrin receptors can be detected in the endosome before they appear on the cell surface. *J. Biol. Chem.* 270:10999-11003.
- Geng, L., Y. Sefal, B. Peissel, N. Deng, Y. Pei, F. Carone, H.G. Rennke, A.M. Glücksmann-Kuis, M.C. Schneider, M. Ericsson, et al. 1996. Identification and localization of polycystin, the PKD1 gene product. *J. Clin. Invest.* 98:2674-2682.
- Geng, L., Y. Segal, A. Pavlova, E.J.G. Barros, C. Löhning, W. Lu, S.K. Nigam, A.-M. Frischauf, S.T. Reeders, and J. Zhou. 1997. Distribution and developmentally regulated expression of murine polycystin. *Am. J. Physiol.* 272:F451-F459.
- Grindstaff, K.K., C. Yeaman, N. Anandasabapathy, S. Hsu, E. Rodriguez-Boulan, R.H. Scheller, and W.J. Nelson. 1998. Sec6/8 complex is recruited to cell-cell contacts and specifies transport vesicle delivery to the basal-lateral membrane in epithelial cells. *Cell.* 93:731-740.
- Gumbiner, B., B. Stevenson, and A. Grimaldi. 1988. The role of the cell adhesion molecule uvomorulin in the formation and maintenance of the epithelial junctional complex. *J. Cell Biol.* 107:1575-1587.
- Harlow, E., and D. Lane. 1988. *Antibodies: A Laboratory Manual.* Cold Spring Harbor Laboratory, Cold Spring Harbor, NY.
- Herz, J., and R.D. Gerard. 1993. Adenovirus-mediated transfer of low density lipoprotein receptor gene acutely accelerates cholesterol clearance in normal mice. *Proc. Natl. Acad. Sci. USA.* 90:2812-2816.
- Huan, Y., and J. van Adelsberg. 1999. Polycystin-1, the PKD1 gene product, is in a complex containing E-cadherin and the catenins. *J. Clin. Invest.* 104:1459-1468.
- Hughes, J., C.J. Ward, B. Peral, R. Aspinwall, K. Clark, M.J.L. San, V. Gamble, and P.C. Harris. 1995. The polycystic kidney disease 1 (PKD1) gene encodes a novel protein with multiple cell recognition domains. *Nat. Genet.* 10:151-160.
- Ibraghimov-Beskrovnaya, O., W.R. Dackowski, L. Foggensteiner, N. Coleman, S. Thiru, L.R. Petry, T.C. Burn, T.D. Connors, T. Van Raay, J. Bradley, et al. 1997. Polycystin: in vitro synthesis, in vivo tissue expression, and subcellular localization identifies a large membrane-associated protein. *Proc. Natl. Acad. Sci. USA.* 94:6397-6403.
- International Polycystic Kidney Disease Consortium. 1995. Polycystic kidney disease: the complete structure of the PKD1 gene and its protein. *Cell.* 81:289-298.
- Koptides, M., C. Hadjimichael, P. Koupepidou, A. Pierides, and C. Constantinou-Deltas. 1999. Germinal and somatic mutations in the PKD2 gene of renal cysts in autosomal dominant polycystic kidney disease. *Hum. Mol. Genet.* 8:509-513.
- Kuchler, R.J. 1977. *Biochemical Methods in Cell Culture and Virology.* Dowden, Hutchinson, and Ross, Stroudsburg, PA.
- Le, T.L., A.S. Yap, and J.L. Stow. 1999. Recycling of E-cadherin: a potential mechanism for regulating cadherin dynamics. *J. Cell Biol.* 146:219-232.
- Le Bivic, A., Y. Sambuy, K. Mostov, and E. Rodriguez-Boulan. 1990. Vectorial targeting of an endogenous apical membrane sialoglycoprotein and uvomorulin in MDCK cells. *J. Cell Biol.* 110:1533-1539.
- Leitinger, B., A. Hille-Rehfeld, and M. Spiess. 1995. Biosynthetic transport of the asialoglycoprotein receptor H1 to the cell surface occurs via endosomes. *Proc. Natl. Acad. Sci. USA.* 92:10109-10113.
- Lipsky, N.G., and R.E. Pagano. 1985. Intracellular translocation of fluorescent sphingolipids in cultured fibroblasts: endogenously synthesized sphingomyelin and glucocerebroside analogues pass through the Golgi apparatus en route to the plasma membrane. *J. Cell Biol.* 100:27-34.
- Lisanti, M.P., A. Le Bivic, M. Sargiacomo, and E. Rodriguez-Boulan. 1989. Steady-state distribution and biogenesis of endogenous Madin-Darby canine kidney glycoproteins: evidence for intracellular sorting and polarized cell surface delivery. *J. Cell Biol.* 109:2117-2127.
- Matlin, K., D.F. Bainton, M. Pesonen, D. Louvard, N. Genty, and K. Simons. 1983. Transepithelial transport of a viral membrane glycoprotein implanted into the apical plasma membrane of Madin-Darby canine kidney cells. I. Morphological evidence. *J. Cell Biol.* 97:627-637.

- Matter, K., W. Hunziker, and I. Mellman. 1992. Basolateral sorting of LDL receptor in MDCK cells: the cytoplasmic domain contains two tyrosine-dependent targeting determinants. *Cell* 71:741-753.
- Mochizuki, T., G. Wu, T. Hayashi, S.L. Xenophontos, B. Veldhuisen, J.J. Saris, D.M. Reynolds, Y. Cai, P.A. Gabow, A. Pierides, et al. 1996. PKD2, a gene for polycystic kidney disease that encodes an integral membrane protein. *Science* 272:1339-1342.
- Moy, G.W., L.M. Mendoza, J.R. Schulz, W.J. Swanson, C.G. Glabe, and V.D. Vacquier. 1996. The sea urchin sperm receptor for egg jelly is a modular protein with extensive homology to the human polycystic kidney disease protein, PKD1. *J. Cell Biol.* 133:809-817.
- Obermüller, N., A.R. Gallagher, Y. Cai, N. Gassler, N. Gretz, S. Somlo, and R. Witzgall. 1999. The rat Pkd2 protein assumes distinct subcellular distribution in different organs. *Am. J. Physiol.* 277:F914-F925.
- Pagano, R.E. 1989. A fluorescent derivative of ceramide: physical properties and use in studying the Golgi apparatus of animal cells. In *Fluorescence Microscopy of Living Cells in Culture*. Y.-I. Wang and D.L. Taylor, editors. Academic Press, San Diego, CA. 75-85.
- Paul, R., C.M. Ewing, J.C. Robinson, F.F. Marshall, K.R. Johnson, M.J. Wheelock, and W.B. Isaacs. 1997. Cadherin-6, a cell adhesion molecule specifically expressed in the proximal renal tubule and renal cell carcinoma. *Cancer Res.* 57:2741-2748.
- Peyrieras, N., F. Hyafil, D. Louvard, H.L. Ploegh, and F. Jacob. 1983. Uvomorulin: a nonintegral membrane protein of early mouse embryo. *Proc. Natl. Acad. Sci. USA.* 80:6274-6277.
- Qian, F., T.J. Watnick, L.F. Onuchic, and G.G. Germino. 1996. The molecular basis of focal cyst formation in human autosomal dominant polycystic kidney disease type I. *Cell* 87:979-987.
- Qian, F., F.J. Germino, Y. Cai, X. Zhang, S. Somlo, and G.G. Germino. 1997. PKD1 interacts with PKD2 through a probable coiled-coil domain. *Nat. Genet.* 16:170-183.
- Rankin, C.A., K. Suzuki, Y. Itoh, D.M. Ziemer, J.J. Grantham, J.A. Calvet, and H. Nagase. 1996. Matrix metalloproteinases and TIMPS in cultured C57BL/6J-cpk kidney tubules. *Kidney Int.* 50:835-844.
- Reeders, S.T., M.H. Breuning, K.E. Davis, R. Nicholls, A. Jarman, D. Higgs, P. Peerson, and D. Weatherall. 1985. A highly polymorphic DNA marker linked to adult polycystic kidney disease on chromosome 16. *Nature.* 317:542-544.
- Scheiffele, P., M.G. Roth, and K. Simons. 1997. Interaction of influenza virus hemagglutinin with sphingolipid-cholesterol membrane domains via its transmembrane domain. *EMBO (Eur. Mol. Biol. Organ.) J.* 16:5501-5508.
- Shimoyama, Y., M. Gotoh, T. Terasaki, M. Kitajima, and S. Hirohashi. 1995. Isolation and sequence analysis of human cadherin-6 complementary DNA for the full coding sequence and its expression in human carcinoma cells. *Cancer Res.* 55:2206-2211.
- Shore, E.M., and W.J. Nelson. 1991. Biosynthesis of the cell adhesion molecule uvomorulin (E-cadherin) in Madin Darby canine kidney epithelial cells. *J. Biol. Chem.* 266:19672-19680.
- Simons, K., and S.D. Fuller. 1985. Cell surface polarity in epithelia. *Annu. Rev. Cell Biol.* 1:243-288.
- Spector, D.L., R. Goldman, and L. Leinwand. 1998. *Cells: A Laboratory Manual*. Cold Spring Harbor Press, Cold Spring Harbor, NY.
- TerBush, D.R., T. Maurice, D. Roth, and P. Novick. 1996. The exocyst is a multi-protein complex required for exocytosis in *Saccharomyces cerevisiae*. *EMBO (Eur. Mol. Biol. Organ.) J.* 15:6483-6494.
- Tsiokas, L., E. Kim, T. Arnould, V.P. Sukhatme, and G. Walz. 1997. Homo- and heterodimeric interactions between the gene products of PKD1 and PKD2. *Proc. Natl. Acad. Sci. USA.* 94:6965-6970.
- Van Driel, I.R., M.S. Brown, and J.L. Goldstein. 1989. Stoichiometric binding of low density lipoprotein (LDL) and monoclonal antibodies to LDL receptors in a solid phase assay. *J. Biol. Chem.* 264:9533-9538.
- van Meer, G., E.H. Stelzer, R.W. Wijnaendts-van-Resandt, and K. Simons. 1987. Sorting of sphingolipids in epithelial (Madin-Darby canine kidney) cells. *J. Cell Biol.* 105:1623-1635.
- Vestweber, D., and R. Kemler. 1984. Some structural and functional aspects of the cell adhesion molecule uvomorulin. *Cell Diff.* 15:269-273.
- Wandinger-Ness, A., M.K. Bennett, C. Antony, and K. Simons. 1990. Distinct transport vesicles mediate the delivery of plasma membrane proteins to the apical and basolateral domains of MDCK cells. *J. Cell Biol.* 111:987-1000.
- Wilson, P.D. 1997. Epithelial cell polarity and disease. *Am. J. Physiol.* 272:F434-F442.
- Wilson, P.D., R.W. Schrier, R.D. Breckon, and P.A. Gabow. 1986. A new method for studying human polycystic kidney disease epithelia in culture. *Kidney Int.* 30:371-378.
- Wilson, P.D., A.C. Sherwood, K. Palla, J. Du, R. Watson, and J.T. Norman. 1991. Reversed polarity of Na⁺-K⁺-ATPase: mislocation to apical plasma membranes in polycystic kidney disease epithelia. *Am. J. Physiol.* 260:F420-F430.
- Wu, G., V. D'Agati, Y. Cai, G. Markowitz, J.H. Park, D.M. Reynolds, Y. Maeda, T.C. Le, H. Hou, Jr., R. Kucherlapati, et al. 1998. Somatic inactivation of PKD2 results in polycystic kidney disease. *Cell* 93:177-188.
- Xiang, Y.Y., M. Tanaka, M. Suzuki, H. Igarashi, E. Kiyokawa, Y. Naito, Y. Ohtawara, Q. Shen, H. Sugimura, and I. Kino. 1994. Isolation of complementary DNA encoding K-cadherin, a novel rat cadherin preferentially expressed in fetal kidney and kidney carcinoma. *Cancer Res.* 54:3034-3041.
- Yeaman, C., A.H. Le Gall, A.N. Baldwin, L. Monlauzeur, A. Le Bivic, and E. Rodriguez-Boulan. 1997. The O-glycosylated stalk domain is required for apical sorting of neurotrophin receptors in polarized MDCK cells. *J. Cell Biol.* 139:929-940.
- Yeaman, C., K.K. Grindstaff, and W.J. Nelson. 1999. New perspectives on mechanisms involved in generating epithelial cell polarity. *Physiol. Rev.* 79:73-98.
- Yoon, S.O., C. Lois, M. Alvarez, A. Alvarez-Buylla, E. Falck-Pedersen, and M.V. Chao. 1996. Adenovirus-mediated gene delivery into neuronal precursors of the adult mouse brain. *Proc. Natl. Acad. Sci. USA.* 93:11974-11979.
- Yoshimori, T., P. Keller, M.G. Roth, and K. Simons. 1996. Different biosynthetic transport routes to the plasma membrane in BHK and CHO cells. *J. Cell Biol.* 133:247-256.